BILINGUAL PUBLISHING CO.
Pioneer of Global Academics Since 1984

Hydro Science & Marine Engineering
https://ojs.bilpublishing.com/index.php/hsme

ARTICLE

Water as the Pore Former in the Synthesis of Hydrophobic PVDF Flat Sheet Membranes for Use in Membrane Distillation

Lebea N. Nthunya[1*] Leonardo Gutierrez[2,3] Edward N. Nxumalo[4] Sabelo D. Mhlanga[5]

1. Department of Chemical, Metallurgical and Material Engineering, Tshwane University of Technology, Private Bag x680, Pretoria, 0001, South Africa
2. Particle and Interfacial Technology Group, Department of Applied Analytical and Physical Chemistry, Ghent University, Coupure Links 653, 9000 Ghent, Belgium
3. Facultad del Mar y Medio Ambiente, Universidad del Pacifico, Guayaquil, Ecuador
4. Nanotechnology and Water Sustainability Research Unit, College of Science, Engineering and Technology, University of South Africa, Florida, 1709, Johannesburg, South Africa
5. DST/MINTEK Nanotechnology Innovation Centre, Strijdom Park, Randburg, 2125, Johannesburg, South Africa

ARTICLE INFO

Article history
Received: 28 October 2019
Accepted: 15 November 2019
Published Online: 30 November 2019

Keywords:
Direct contact membrane distillation
PVDF flat sheet membranes
Superhydrophobic silica nanoparticles
Water as the pore former

ABSTRACT

Although PVDF flat sheet membranes have been widely tested in MD, their synthesis and modifications currently require increased use of green and inexpensive materials. In this study, flat sheet PVDF membranes were synthesized using phase inversion and water as the pore former. Remarkably, the water added in the casting solution improved the membrane pore sizes; where the maximum pore size was 0.58 µm. Also, the incorporation of f-SiO2NPs in the membrane matrix considerably enhanced the membrane hydrophobicity. Specifically, the membrane contact angles increased from 96° to 153°. Additionally, other parameters investigated were mechanical strength and liquid entry pressure (LEP). The maximum recorded values were 2.26 MPa and 239 kPa, respectively. The modified membranes (i.e., using water as the pore former and f-SiO2NPs) were the most efficient, showing maximum salt rejection of 99.9% and water flux of 11.6 LMH; thus, indicating their capability to be used as efficient materials for the recovery of high purity water in MD.

1. Introduction

Although water is a crucial component of life, water scarcity and pollution continue to threaten humans, and every living organism and ecosystem on the planet [1,2]. Nearly 1.1 billion people lack access to fresh and clean water [3–5]. These water challenges are commonly observed in rural settlements in developing countries [1,6,7]. Currently, wastewater reuse and desalination serve as suitable alternatives to meet the increasing demand for clean water, and to tackle water shortages. Desalination has been extensively studied using membrane technology [8,9]. Notably, Membrane Distillation (MD) has attracted the interest of many researchers over other membrane technologies due to its efficient removal of salts from water [10–12].

**Corresponding Author:*
Lebea N. Nthunya,
Department of Chemical, Metallurgical and Material Engineering, Tshwane University of Technology, Private Bag x680, Pretoria, 0001, South Africa;
Email: NthunyaLN@tut.ac.za / nthunyalebea@gmail.com

 DOI: https://doi.org/10.30564/hsme.v1i2.1346

Membrane distillation is a liquid-mixture separation process through a hydrophobic membrane. The vapour pressure gradient induced by the temperature difference across the two interfaces of the membranes is the main driving force of the process [13–16]. Therefore, the water is transported through the porous membrane in the form of vapour. In addition to process parameters and module designs, MD performance is affected by membrane morphology (i.e., including size and distribution of pores, porosity, and surface roughness), physical and chemical characteristics of the membrane, as well as membrane wettability. Among other challenges, membrane morphology has been the most limiting factor in simultaneously controlling membrane wetting as well as improved fluxes [17–20].

To circumvent the low rates of water recoveries in MD, several studies have focused on the improvement of the membrane pore sizes. Briefly, the electrospinning of nanofibre membranes has been tested as an alternative technique to enhance membrane pore sizes, pore distribution, and porosity [21–24]. However, the resulting membranes were prone to fouling owing to their high surface roughness [10,25–28]. Similarly, highly porous membranes (i.e., pore sizes > 1.5 μm) have shown a negative impact on the Liquid Entry Pressure (LEP) of the membrane. Putting this into a technical perspective, the LEP of membranes must be strictly higher than the MD operating pressures [29,30]. Consequently, nanofibre membranes are likely to encourage the passage of liquid water due to their large pores; thus, compromising the overall performance of the separation process [30,31].

Besides nanofibre membranes, flat sheet and hollow fiber membranes have been extensively explored for their possible application in MD. For instance, Bruggen and co-workers tested commercial PTFE, PVDF, PE, and PP flat sheet membranes in Direct-Contact MD (DCMD)[32]. Water fluxes ranging between 15 – 20 $L \cdot m^{-2} \cdot h^{-1}$ were reported. Several water-soluble pore-forming agents, including polyvinyl pyrrolidone (PVP), polyethylene glycol (PEG), and polyacrylic acid (PAA) have been successfully tested for enhancing the pores of the membrane [33]. Although water is a green component during membrane synthesis, its exploitation in the preparation of MD membranes has been rarely reported. In this study, water was used as the pore former (additive) and non-solvent (coagulant) during the phase-inversion synthesis of hydrophobic PVDF flat sheet membranes for MD. Moreover, octadecyltrimethoxysilane (OTMS)-modified silica nanoparticles (f-SiO_2NPs) were incorporated into the PVDF membranes to enhance their hydrophobicity. This novel combined procedure would highly assist in preventing MD membrane wetting, improving the rate of water recovery, as well as increasing salt rejections.

2. Materials and Methods

2.1 Reagents

PVDF (MW = 534,000 g mol^{-1}), *N,N*-dimetheylacetamide (DMAc) (Puriss p.a., 99.5%) were purchased from Sigma Aldrich (Germany). Deionized water (Direct-Q®, Merck Millipore) were used for solution preparation.

2.2 Synthesis of Membrane Samples

PVDF flat sheet membranes were prepared following a previously reported non-solvent induced phase method [34]. Briefly, PVDF (10 g) was transferred to a conical flask containing DMAc (100 mL). In order to enhance the membrane pore sizes and hydrophobicity, water and OTMS-modified SiO_2NPs were added into the casting solution. The detailed synthesis of OTMS-modified SiO_2NPs is reported elsewhere [35]. The mixtures were stirred for 4 h at 80°C, followed by vacuum degassing. The compositions of the casting solutions are presented in Table 1. The solutions were cast on a glass plate using a casting knife with a gap height of 150 μm, followed by immediate immersion in a 15°C water coagulation bath. The prepared membranes were stored in deionized water for 48 h to complete the phase separation process. The membranes were air-dried prior to characterization and use. Pristine PVDF flat sheet membranes (i.e., neither pore-enhanced nor modified with f-SiO_2NPs) were termed as M1. The pore-enhanced membranes using 2% and 4% water additive were termed as M2 and M3, respectively. Similarly, the pore-enhanced membranes using 2% and 4% water additive and subsequently modified with 1%(w/v) f-SiO_2NPs were termed as M4 and M5, respectively.

Table 1. Composition of the casting solution for the synthesis of PVDF flat sheet membranes

Membrane	PVDF (g)	DMAc (mL)	H_2O (g)	SiO_2NPs (g)
M1	10	100	0	0
M2	10	100	2	0
M3	10	100	4	0
M4	10	100	2	0.1
M5	10	100	4	0.1

2.3 Characterization of Membranes

The surface and cross-sectional morphology of the membranes were investigated using Scanning Electron Microscopy (SEM, JOEL STM-IT300). Likewise, the surface to-

DOI: https://doi.org/10.30564/hsme.v1i2.1346

pography and roughness of the membranes were analyzed using Atomic Force Microscopy (AFM, Witec Alpha 300 A, TS-150). In order to assess the hydrophobic nature of the membranes, water contact angle measurements were conducted using the sessile drop method in a DSA3OE Kruss drop shape analyzer (GnbH). The Liquid Entry Pressure (LEP) was measured using a dead-end cell. The cell was filled with deionized water, and the pressure was gradually increased until the presence of filtrate was recorded. The tensile strengths of the membranes were calculated from the stress-strain graphs, which were obtained using a Small Angle X-ray Scattering system (SAXSpace, Anton Paar GmbH) equipped with a universal extensional fixture. The membrane pore sizes were measured using the dry-to-wet method in a liquid expulsion capillary flow porometer (3G). Finally, the porosity of the membranes was obtained from the polymer density measurements where isopropyl alcohol (i.e., which penetrates inside the pores of the membrane) and de-ionized water (i.e., which does not penetrate through the membrane pores) were used. The following equation was used to calculate the membrane porosity (ε).

$$\varepsilon = \frac{(w_w - w_d)/\rho_i}{(w_w - w_d)/\rho_i + w_d/\rho_p} \quad (1)$$

Where w_d is the weight of the dry membrane, w_w is the weight of the wet membrane, ρ_i is the density of isopropyl alcohol, and ρ_p is the density of the polymer.

2.4 Membrane performance in Direct Contact Membrane Distillation

The performance of the PVDF flat sheet membranes was studied on a DCMD laboratory-scale set-up using a 35%(w/v) NaCl solution (i.e., typical concentration of dissolved salts in seawater). The temperature of the feed and permeate streams were kept at 60°C and 20°C, respectively. The feed and permeate streams were cycled through the MD cell (i.e., active surface area of 1.25×10^{-2} m^2) at a flow rate of 0.75 L·min^{-1} in a counter flow mode. The feed stream was composed of either deionized water (i.e., resistivity of 18 MΩ.cm) or saline water (i.e. 35%(w/v) NaCl solution), while the initial permeate stream was composed of deionized water. The water flux was calculated using equation 2, by following the change in permeate weight (g) over time. The weight increment of the water passing through the membrane in vapour state was measured using an EMB 3000_1 weighing balance (Kern & Sohn GmbH). To calculate the salt rejection efficiency, the conductivity of the feed and permeate solutions was monitored using a Shimadzu conductivity meter. Based on the initial and final electrical conductivities of the feed and the permeate, equation 4 was used to calculate the salt rejection (*SR*) performance.

$$J_{water} = \frac{\Delta V}{\Delta t \cdot A} \quad (2)$$

Where ΔV is the volume of the permeate collected at a time interval Δt, and A_m is the membrane surface area. The difference in volume (ΔV) was calculated from the change in mass (Δm) of the water collected, where 0.997 kg/L was used as the density (ρ) of water at room temperature (equation 3).

$$\Delta V = \frac{\Delta m}{\rho} \quad (3)$$

$$SR = \left(1 - \frac{C_p}{C_f}\right) * 100\% \quad (4)$$

Where *SR* is the salt rejection, C_f and C_p are the salt concentrations in the feed and permeate streams, respectively.

3. Results and Discussion

3.1 Morphological Analysis of Membranes

The SEM analysis was performed to investigate the surface morphology and pore geometry of the PVDF flat sheet membranes. Figure 1 presents the surface and cross-sectional micrographs of the membranes. All membranes exhibited similar topography with a slight change in pore size when the amount of pore former (water) was increased in the casting solution. The differences in membrane pore sizes were discussed in the forthcoming sections. During the preparation of the casting solution, the maximum amount of water added was 4%(w/w) relative to the solution. Beyond this weight percentage, the casting solution formed a suspension due to the exchange of solvent (DMAc) and non-solvent (water). Remarkably, the porous structure of the membrane was formed when the coagulation processed was slowed down. Therefore, the added water during the preparation of the casting solution reduced the diffusion rate of the non-solvent during phase separation.

A careful analysis of the cross-sectional images demonstrated the formation of finger-like pore structures. Remarkably, the interstitial spaces between the porous

 DOI: https://doi.org/10.30564/hsme.v1i2.1346

internal structures increased with increasing water content (Figure 1 M2-M5). Similar observations were reported by Malik et al. (2018) when water-soluble polymers such as PAA and PEG were used as pore formers during membrane synthesis [33]. Contrarily, the addition of f-SiO_2NPs did not show a significant change in surface and internal morphology. Therefore, the water added as an additive in the casting solution played a significant contribution in the formation of the microvoids within the internal structure of the membrane. According to Gumbi and co-workers, water increases the casting viscosity; thus, bringing the solution viscosity closer to the binodal composition where the suppression of macrovoids is favoured [34]. These changes in membrane morphology as a function of increase in additive content have a direct impact on membrane topology and roughness [36].

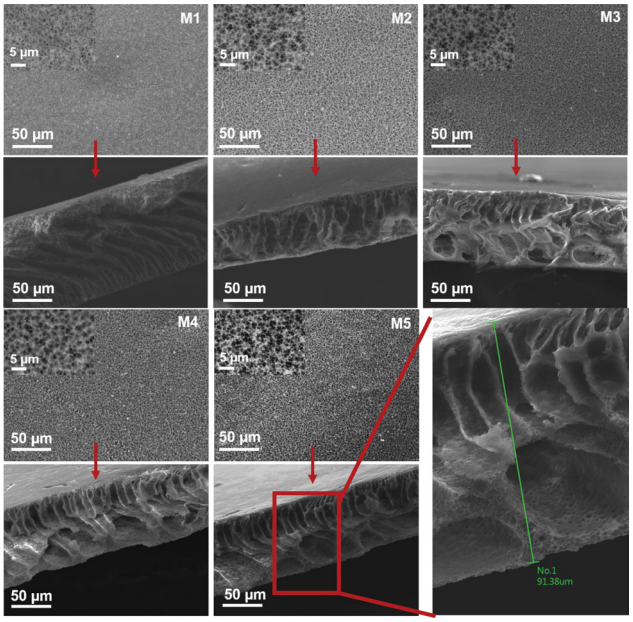

Figure 1. SEM micrographs of PVDF flat sheet membranes

Note: (M1) Pristine PVDF flat sheet membranes, (M2 & M3) pore-enhanced membranes using 2% and 4% water additive, respectively, and (M4 & M5) pore-enhanced membranes using 2% and 4% water additive, respectively, and subsequently modified with 1%(w/v) f-SiO_2NPs.

To investigate the effect of additives (i.e., water and f-SiO_2NPs) on the membrane topology and roughness, an AFM analysis of the membranes was conducted (Figure 2). The analysis was performed on pristine PVDF flat sheet membranes (M1), pore-enhanced membranes using 4% water additive (M3), and pore-enhanced membranes using 4% water additive and subsequently modified with 1%(w/v) f-SiO_2NPs (M5). These membranes selected for AFM characterization are a representative of the different synthesis methods performed in the current study. The surface roughness increased upon addition of water in the casting solution, as evidenced by the root mean square roughness ($Sq_{M1} < Sq_{M2}$). Likewise, the addition of f-SiO_2NPs further enhanced the membrane surface roughness. Thus, the order of membrane surface roughness was M1<M3<M5. Remarkably, the increase in membrane roughness was not only caused by the pore formation induced by water added as an additive in the casting solution but also by the membrane viscosity as stated in the previous section. Additionally, surface roughness was mainly caused by the protrusion of SiO_2NPs leading to the formation of re-entrant structures. In previous studies, it was reported that membranes with high surface roughness encourage air-entrapment [26]. These air-entrapment increases membrane resistance to wetting by low surface tension liquids. An increase in membrane roughness is an indication of increased effective membrane area caused by the nodular shapes with valleys, which is ultimately beneficial for MD applications.

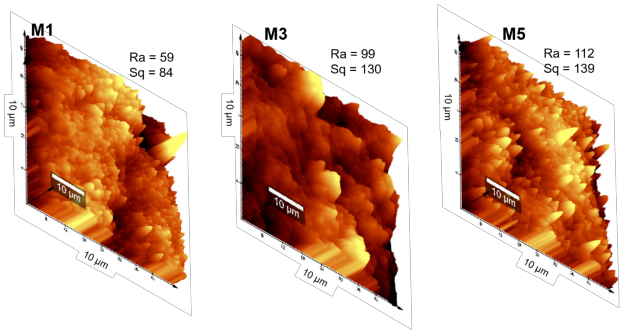

Figure 2. AFM images of PVDF flat sheet membranes

Note: (M1) Pristine PVDF flat sheet membranes without the pore former and SiO_2NPs, (M3) pore-enhanced membranes using 4% water additive, and (M5) pore-enhanced membranes using water 4% water additive and subsequently modified with 1%(w/v) f-SiO_2NPs.

3.2 Contact Angles and Liquid Entry Pressure

The membranes used in MD applications should be strictly porous and not be wetted by the process liquids [10]. Consequently, the LEP should not be lower than the operating pressure of the process. Therefore, the membranes should be hydrophobic. As such, the effect of additives on the membrane wettability (i.e., assessed by the membrane contact angle) and liquid entry pressure were presented in Figure 3. The contact angle (CA) results showed that the pristine PVDF flat sheet membranes (M1) were hydrophobic (CA = 96±2°). The addition of water as the pore former did not impact the membrane contact angles. The contact angles for M1, M2, and M3 were approximately similar (CA_{M1} = 96°, CA_{M2} = 97°, CA_{M3} = 94°). Remarkably, the PVDF membranes changed from hydrophobic to superhydrophobic (CA ≈ 153°) upon the addition of f-SiO_2NPs. This phenomenon was in agreement with pre-

DOI: https://doi.org/10.30564/hsme.v1i2.1346

viously reported studies [37,38].

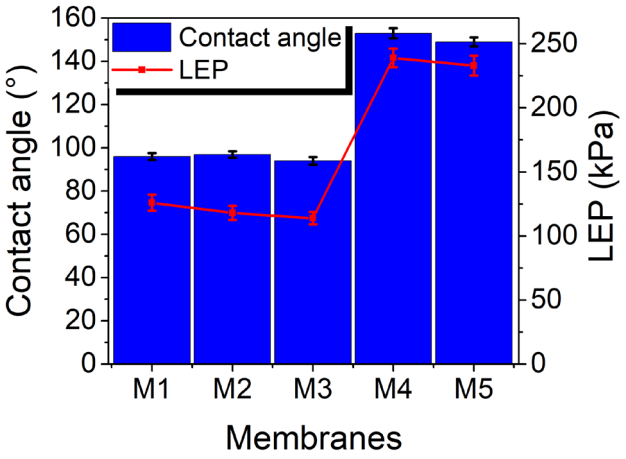

Figure 3. Contact angles and LEP of PVDF flat sheet membranes

Note: (M1) Pristine PVDF flat sheet membranes, (M2 & M3) pore-enhanced membranes using 2% and 4% water additive, respectively, and (M4 & M5) pore-enhanced membranes using 2% and 4% water additive, respectively, and subsequently modified with 1%(w/v) f-SiO_2NPs.

The membrane-water contact angle showed a direct impact on the liquid entry pressure (LEP). Also, the LEP was affected by the membrane pore size as well as the geometry. Notably, the LEP gradually decreased from 126 kPa (M1) to 114 kPa (M3). This change in LEP was ascribed to the increase in membrane pore-size (Figure 4). A drastic change in LEP (i.e. from 126 kPa to 239 kPa) was observed on the superhydrophobic membranes (i.e., compared to the hydrophobic membranes). This change was caused by cavitation induced by the superhydrophobic nature of the membranes and the water polarity. Water becomes energetically unstable when in contact with the superhydrophobic membranes, resulting in the formation of water bubbles and blocking the membrane pores. Consequently, the water requires higher pressures to be driven across the membrane. This phenomenon was also reported by Li and co-workers [39].

3.3 Pore Size and Mechanical Strength of Membranes

As previously indicated, membrane pore sizes have a direct relationship with LEP. Similarly, the membrane pores also exert an impact on the mechanical strength of the membrane. Therefore, to investigate the effect of additives on the size of the pores and the mechanical strength of membranes, the membrane pore size and Young's modulus were recorded and presented in Figure 4. The pore sizes of membranes M1, M2, M3, M4, and M5 were 0.21 µm, 0.39 µm, 0.52 µm, 0.47 µm, and 0.58 µm, respectively. The size of the membrane pores depends on the rate of solution phase separation. Briefly, the addition of the pore former (water) decreased the rate of solvents exchange during phase separation leading to the formation of big pores. Therefore, water was the primary contributing factor for the formation of highly porous membranes.

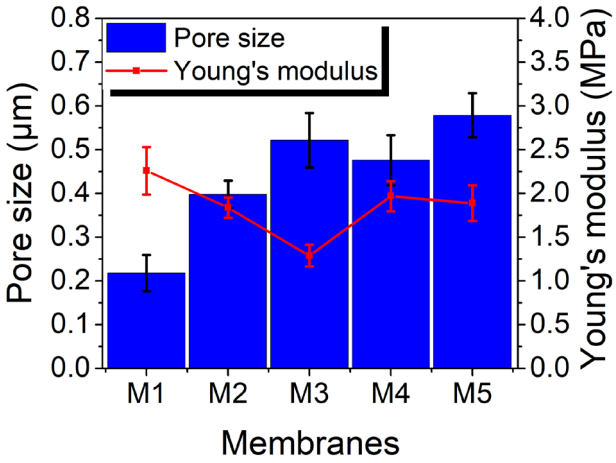

Figure 4. Pore size and Young's modulus of PVDF flat sheet membranes

Note: (M1) Pristine PVDF flat sheet membranes, (M2 & M3) pore-enhanced membranes using 2% and 4% water additive, respectively, and (M4 & M5) pore-enhanced membranes using 2% and 4% water additive, respectively, and subsequently modified with 1%(w/v) f-SiO_2NPs.

While highly porous membranes are a pre-requisite in MD, the increase in membrane pores led to a decrease in mechanical strength, as evidenced by Young's modulus (Figure 4). Specifically, Young's moduli decreased from 2.26 MPa for the pristine membrane (M1) to 1.29 MPa upon the addition of 4% H_2O in the casting solution (M3). This lower mechanical strength was associated with increased voids within the structure, causing a crack propagation during tensile stress and subsequently resulting in a mechanically weaker membrane. However, further addition of f-SiO_2NPs led to a slight increase in mechanical strength. The incorporation of NPs in the membrane decreased the membrane porosity, rendering them stronger. Also, the silica nanoparticles act as crosslinkers in the composite membranes and increase the membrane rigidity, which subsequently improved their mechanical strength. Similar observations have been reported elsewhere [38,39].

3.4 Flux and salt rejection studies

The water flux and salt rejection across all PVDF flat sheet membranes were studied in a DCMD set-up, and the results were presented in Figure 5 and 6, respectively. The measurements were conducted at 10 h. intervals while the feed and permeate temperatures were kept at 60° and 20°, respectively. The initial water fluxes of M1, M2, M3, M4, and M5 were 6.6 LMH, 7.8 LMH, 8.2 LMH, 10.2 LMH,

 DOI: https://doi.org/10.30564/hsme.v1i2.1346

and 11.6 LMH, respectively. An unstable slight increase in water flux on M1, M2, and M3 was associated with the possible wetting within membranes; thus, promoting the passage of water in a liquid state. This possible membrane wetting would be related to low LEP values (114-126 kPa). Thus, the final water flux on M1-M3 ranged between 6.9 LMH – 8.1 LMH. Contrariwise, an unstable slight decrease in water flux was observed on M4 and M5. This flux decay was attributed to the possible temperature polarization and membrane artifacts deviations. The final water flux on M4 and M5 was 9.4 LMH and 9.7 LMH, respectively. Although the superhydrophobic membranes (M4-M5) were affected by the process parameters, resulting in a flux decay as a function of time, they performed well in terms of fluxes compared to the less hydrophobic M1-M3.

The salt rejection studies were performed using 35%(w/v) NaCl. A 99.9% salt rejection was recorded for f-SiO_2NPs-modified PVDF flat sheet membranes. An almost stable salt rejection was observed with a minimal loss (≤0.06%) on M4 and M5. Furthermore, a slight loss in salt rejection (from 99.2% to 97.8%) was recorded on pristine PVDF membrane (M1). Salt rejection losses recorded for M1-M3 were in the range of 1.4-1.5%. The higher decay in salt rejection on M1-M3 compared to M4-M5 would be attributed to membrane wetting. While membrane porosity is a requirement in MD, highly porous membranes with low hydrophobicity promote membrane wetting by the process liquids; thus, compromising the separation efficiency of the membrane. Therefore, a combined strategy for improved membrane porosity and hydrophobicity is imperative.

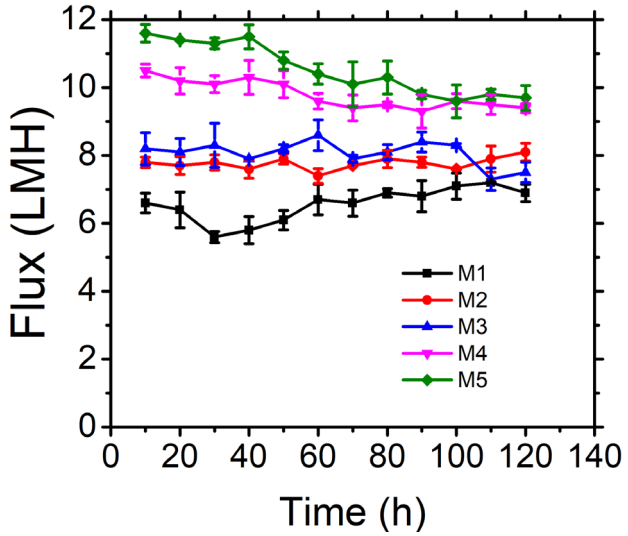

Figure 5. Water flux in DCMD using PVDF flat sheet membranes

Note: (M1) Pristine PVDF flat sheet membranes, (M2 & M3) pore-enhanced membranes using 2% and 4% water additive, respectively, and (M4 & M5) pore-enhanced membranes using 2% and 4% water additive, respectively, and subsequently modified with 1%(w/v) f-SiO_2NPs.

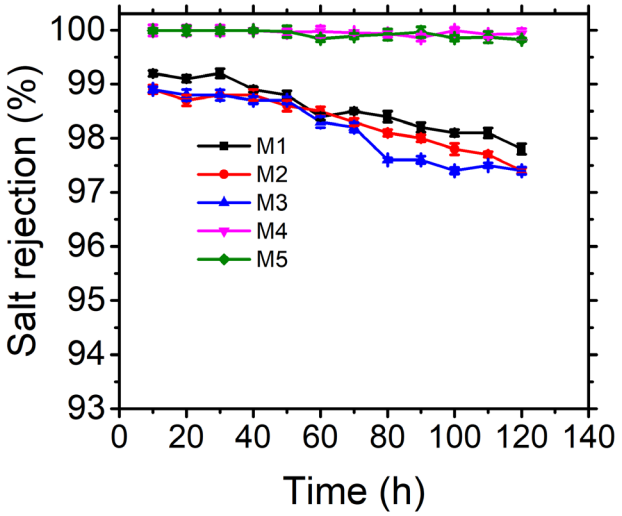

Figure 5. Salt rejection in DCMD using PVDF flat sheet membranes

Note: (M1) Pristine PVDF flat sheet membranes, (M2 & M3) pore-enhanced membranes using 2% and 4% water additive, respectively, and (M4 & M5) pore-enhanced membranes using 2% and 4% water additive, respectively, and subsequently modified with 1%(w/v) f-SiO_2NPs.

3.5 Membrane Performance Comparison Studies

A comparison of MD performance using PVDF flat sheet membranes was illustrated in Table 2. This summary was obtained from the literature and the current study. The synthesized PVDF flat sheet membranes demonstrated performances similar to those in the literature. The highest flux (22.4 LHM) was reported by Fan et al (2013) [40]. However, the salt rejection reported were similar to those obtained from the f-SiO_2NPs reported in the current study.

Table 2. Properties of PVDF membranes and their performances at 60°C feed temperature

Membrane	Thickness (µm)	CA (°)	LEP (kPa)	Pore size (µm)	Porosity (%)	Youngs modulus (MPa)	Flux (LMH)	Rejection (%)	Ref.
M1	101.3	96	126	0.22	76	2.3	6.6	99.2	This study
M2	73.4	97	118	0.39	81	1.8	7.8	98.9	This study
M3	94.2	94	114	0.52	86	1.3	8.2	98.9	This study
M4	90.5	153	239	0.47	78	2.0	10.2	99.9	This study
M5	91.3	141	233	0.58	79	1.9	11.6	99.9	This study
PVDF/SiO_2	-	135	310	-	-	-	2.9	99.9	[41]
PVDF/SiO_2	-	156	275	0.52	69	-	8.3	99.9	[42]

DOI: https://doi.org/10.30564/hsme.v1i2.1346

PVDF/ PTFE	81	145	120	0.43	80	-	22.4	99.9	[40]
PVDF	62	-	300	0.34	79	-	5.2	-	[43]
PVDF	104	87	-	0.48	54	-	12	-	[44]
PVDF/ LiCl	-	107	290	-	81	-	9.7	99	[45]

4. Conclusion

In this study, highly porous and superhydrophobic PVDF flat sheet membranes were synthesized and tested for water desalination in MD. The addition of water in the casting solution resulted in improved membrane pores. To achieve superhydrophobicity, f-SiO_2NPs were incorporated in the flat sheet nanocomposite membranes. Remarkably, the NPs did not affect the membrane pore sizes, clearly demonstrating the combined achievement of membrane pores and hydrophobicity for improved application in MD. The recorded membranes pore sizes, mechanical strength, LEP, contact angle were in the following ranges; 0.21-0.58 μm, 1.29-2.26 MPa, 114-239 kPa and 96-153°, respectively. These membranes were efficient in salt rejection. However, the f-SiO_2NPs-modified membranes showed the highest efficiencies. Furthermore, the modified PVDF membranes were characterized by high water fluxes, indicating a promising use for high rate water recoveries in MD.

Declaration

The authors declare no conflict of interest.

Acknowledgment

The authors would like to acknowledge the South African National Research Foundation for funding this work.

References

[1] L.N. Nthunya, M.L. Masheane, S.P. Malinga, E.N. Nxumalo, B.B. Mamba, S.D. Mhlanga, Determination of toxic metals in drinking water sources in the Chief Albert Luthuli Local Municipality in Mpumalanga, South Africa, Phys. Chem. Earth, 2017, 100: 94–100.
DOI: 10.1016/j.pce.2017.04.006

[2] A.Y. Hoekstra, M.M. Mekonnen, A.K. Chapagain, R.E. Mathews, B.D. Richter, Global monthly water scarcity: Blue water footprints versus blue water availability, PLoS One, 2012, 7: 1–9.
DOI: 10.1371/journal.pone.0032688

[3] J.N. Edokpayi, E.T. Rogawski, D.M. Kahler, C.L. Hill, C. Reynolds, E. Nyathi, J.A. Smith, J.O. Odiyo, A. Samie, P. Bessong, R. Dillingham, Challenges to sustainable safe drinking water: A case study ofwater quality and use across seasons in rural communities in Limpopo Province, South Africa, Water (Switzerland), 2018, 10: 1–18.
DOI: 10.3390/w10020159

[4] T. Pradeep, Noble metal nanoparticles for water purification: A critical review, Thin Solid Films, 2009, 517: 6441–6478.
DOI: 10.1016/j.tsf.2009.03.195

[5] R.K. Mishra, S.C. Dubey, Fresh water availability and it's global challenge, Int. J. Eng. Sci. Invent. Res. Dev. 2015, 2: 351–407.

[6] L.N. Nthunya, S. Maifadi, B. Mamba, Bhekie, A.R. Verliefde, S.D. Mhlanga, Spectroscopic determination of water salinity in brackish surface water in Nandoni Dam, at Vhembe District, Limpopo Province, South Africa, Water. 2018, 10: 1–13.
DOI: 10.3390/w10080990

[7] L.N. Nthunya, N.P. Khumalo, A.R. Verliefde, B.B. Mamba, S.D. Mhlanga, Quantitative analysis of phenols and PAHs in the Nandoni Dam in Limpopo Province, South Africa: A preliminary study for dam water quality management, Phys. Chem. Earth, Parts A/B/C, 2019: 1–9.
DOI: 10.1016/j.pce.2019.02.003

[8] G.W. Meindersma, C.M. Guijt, A.B. de Haan, Desalination and water recycling by air gap membrane distillation, Desalination, 2006, 187: 291–301.
DOI: 10.1016/j.desal.2005.04.088

[9] B. van der Bruggen, Desalination by distillation and by reverse osmosis — trends towards the future, Membr. Technol, 2003, 2003: 6–9.
DOI: 10.1016/S0958-2118(03)02018-4

[10] L.N. Nthunya, L. Gutierrez, S. Derese, N. Edward, A.R. Verliefde, B. Mamba, S.D. Mhlanga, A review of nanoparticle-enhanced membrane distillation membranes : membrane synthesis and applications in water treatment, Chem. Technol. Biotechnol, 2019, 94: 2757–2771.
DOI: 10.1002/jctb.5977

[11] A. Alkhudhiri, N. Darwish, N. Hilal, Membrane distillation: A comprehensive review, Desalination, 2012, 287: 2–18.
DOI:10.1016/j.desal.2011.08.027

[12] L. Eykens, K. De Sitter, C. Dotremont, L. Pinoy, B. Van Der Bruggen, How to optimize the membrane properties for membrane distillation: A review, Ind. Eng. Chem. Res. 2016, 55: 9333–9343.
DOI: 10.1021/acs.iecr.6b02226

[13] C. Chiam, R. Sarbatly, Vacuum membrane distillation processes for aqueous solution treatment - A review, Chem. Eng. Process. Process Intensif, 2013, 74: 27–54.

 DOI: https://doi.org/10.30564/hsme.v1i2.1346

DOI: 10.1016/j.cep.2013.10.002

[14] B.L. Pangarkar, S.K. Deshmukh, V.S. Sapkal, R.S. Sapkal, Review of membrane distillation process for water purification, Desalin. Water Treat. 2016, 57: 1–23.
DOI: 10.1080/19443994.2014.985728

[15] L.D. Tijing, Y.C. Woo, J.S. Choi, S. Lee, S.H. Kim, H.K. Shon, Fouling and its control in membrane distillation-A review, J. Memb. Sci. 2015, 475: 215–244.
DOI: 10.1016/j.memsci.2014.09.042

[16] E. Curcio, E. Drioli, Membrane distillation and related operations—A review, Sep. Purif. Rev. 2005, 34: 35–86.
DOI: 10.1081/SPM-200054951

[17] Y. Huang, Z. Wang, J. Jin, S. Lin, Novel Janus Membrane for Membrane Distillation with Simultaneous Fouling and Wetting Resistance, Environ. Sci. Technol, 2017, 51: 13304–13310.
DOI: 10.1021/acs.est.7b02848

[18] Y. Zhang, X. Wang, Z. Cui, E. Drioli, Z. Wang, Enhancing wetting resistance of poly (vinylidene fluoride) membranes for vacuum membrane distillation, Desalination, 2017, 415: 58–66.
DOI: 10.1016/j.desal.2017.04.011

[19] Y. Huang, Z. Wang, D. Hou, S. Lin, Coaxially electrospun super-amphiphobic silica-based membrane for anti- surfactant-wetting membrane distillation, J. Memb. Sci. 2017, 531: 122–128. DOI: 10.1016/j.memsci.2017.02.044

[20] L. Eykens, K. De Sitter, C. Dotremont, W. De Schepper, L. Pinoy, B. Van Der Bruggen, Wetting Resistance of Commercial Membrane Distillation Membranes in Waste Streams Containing Surfactants and Oil, Appl. Sci. 2017, 7: 118.
DOI: 10.3390/app7020118

[21] Y. Chul, L.D. Tijing, W. Shim, J. Choi, S. Kim, T. He, E. Drioli, H. Kyong, Water desalination using graphene-enhanced electrospun nano fiber membrane via air gap membrane distillation, J. Memb. Sci. 2016, 520: 99–110.
DOI: 10.1016/j.memsci.2016.07.049

[22] H. Attia, S. Alexander, C.J. Wright, N. Hilal, Superhydrophobic electrospun membrane for heavy metals removal by air gap membrane distillation (AGMD), Desalination. 2017, 420: 318–329.
DOI: 10.1016/j.desal.2017.07.022

[23] E. Lee, A. Kyoungjin, T. He, Y. Chul, H. Kyong, Electrospun nano fiber membranes incorporating fluorosilane-coated TiO2 nanocomposite for direct contact membrane distillation, 2016, 520: 145–154.
DOI: 10.1016/j.memsci.2016.07.019

[24] Y. Liao, R. Wang, A.G. Fane, Engineering superhydrophobic surface on poly (vinylidene fluoride) nano fiber membranes for direct contact membrane distillation, J. Memb. Sci. 2013, 440: 77–87.
DOI: 10.1016/j.memsci.2013.04.006

[25] L.N. Nthunya, L. Gutierrez, S. Derese, B.B. Mamba, Adsorption of phenolic compounds by polyacrylonitrile nano fi bre membranes : A pretreatment for the removal of hydrophobic bearing compounds from water, J. Environ. Chem. Eng. 2019, 7: 103254.
DOI: 10.1016/j.jece.2019.103254

[26] L.N. Nthunya, L. Gutierrez, R. Verliefde, S.D. Mhlanga, Enhanced flux in direct contact membrane distillation using superhydrophobic PVDF nanofibre membranes embedded with organically modified SiO2 nanoparticles, Chem. Technol. Biotechnol, 2019, 94: 2826–2837.
DOI: 10.1002/jctb.6104

[27] L.N. Nthunya, L. Gutierrez, L. Lapeire, K. Verbeken, N. Zaouri, E.N. Nxumalo, B.B. Mamba, A.R. Verliefde, S.D. Mhlanga, Fouling resistant PVDF nanofibre membranes for the desalination of brackish water in membrane distillation, Sep. Purif. Technol. 2019, 228: 115793.
DOI: 10.1016/j.seppur.2019.115793

[28] L.N. Nthunya, L. Gutierrez, N. Khumalo, S. Derese, B.B. Mamba, A.R. Verliefde, S.D. Mhlanga, Superhydrophobic PVDF nanofibre membranes coated with an organic fouling resistant hydrophilic active layer for direct-contact membrane distillation, Colloids Surfaces A Physicochem. Eng. Asp. 2019, 575: 363–372.
DOI: 10.1016/j.colsurfa.2019.05.031

[29] J. Xu, Y.B. Singh, G.L. Amy, N. Ghaffour, Effect of operating parameters and membrane characteristics on air gap membrane distillation performance for the treatment of highly saline water, J. Memb. Sci. 2016, 512: 73–82.
DOI: 10.1016/j.memsci.2016.04.010

[30] Y.G. Zmievskii, Determination of critical pressure in membrane distillation process, Pet. Chem, 2015, 55: 308–314.
DOI: 10.1134/S0965544115040118

[31] A. Alkhudhiri, N. Hilal, Air gap membrane distillation: A detailed study of high saline solution, Desalination, 2017, 403: 179–186.
DOI: 10.1016/j.desal.2016.07.046

[32] L. Eykens, K. De Sitter, C. Dotremont, L. Pinoy, B. Van der Bruggen, Characterization and performance evaluation of commercially available hydrophobic membranes for direct contact membrane distillation, Desalination, 2016, 392: 63–73.

DOI: https://doi.org/10.30564/hsme.v1i2.1346

DOI: 10.1016/j.desal.2016.04.006

[33] T. Malik, H. Razzaq, S. Razzaque, H. Nawaz, A. Siddiqa, M. Siddiq, S. Qaisar, Design and synthesis of polymeric membranes using water-soluble pore formers : an overview, Polym. Bull, 2018, 76: 4879–4901.
DOI: 10.1007/s00289-018-2616-3

[34] N.N. Gumbi, M. Hu, B.B. Mamba, J. Li, E.N. Nxumalo, Macrovoid-free PES/SPSf/O-MWCNT ultrafiltration membranes with improved mechanical strength, antifouling and antibacterial properties, J. Memb. Sci. 2018, 566: 288–300.
DOI: 10.1016/j.memsci.2018.09.009

[35] L.N. Nthunya, L. Gutierrezb, A.R. Verliefde, S.D. Mhlanga, Enhanced flux in direct contact membrane distillation using superhydrophobic PVDF nanofibre membranes embedded with organically modified SiO2 nanoparticles, J. Chem. Technol. Biotechnol, 2019, 94: 2826–2837.
DOI: 10.1002/jcbt.6104

[36] T.A. Otitoju, A.L. Ahmad, B.S. Ooi, Polyvinylidene fluoride (PVDF) membrane for oil rejection from oily wastewater : A performance review, J. Water Process Eng. 14 (2016) 41–59. DOI: 10.1016/j.jwpe.2016.10.011

[37] D. Hou, D. Lin, C. Ding, D. Wang, J. Wang, Fabrication and characterization of electrospun superhydrophobic PVDF- HFP / SiNPs hybrid membrane for membrane distillation, Sep. Purif. Technol. 2017, 189: 82–89.
DOI: 10.1016/j.seppur.2017.07.082

[38] Z.-Q. Dong, X.-H. Ma, Z.-L. Xu, Z.-Y. Gu, Superhydrophobic modification of PVDF–SiO2 electrospun nanofiber membranes for vacuum membrane distillation, RSC Adv. 2015, 5: 67962–67970.
DOI: 10.1039/C5RA10575G

[39] X. Li, X. Yu, C. Cheng, L. Deng, M. Wang, X. Wang, Electrospun Superhydrophobic Organic/Inorganic Composite Nanofibrous Membranes for Membrane Distillation, ACS Appl. Mater. Interfaces. 2015, 7: 21919–21930.
DOI: 10.1021/acsami.5b06509

[40] H. Fan, Y. Peng, Z. Li, P. Chen, Q. Jiang, S. Wang, Preparation and characterization of hydrophobic PVDF membranes by vapor-induced phase separation and application in vacuum membrane distillation, J. Polym. Res. 2013, 134: 1–15.
DOI: 10.1007/s10965-013-0134-4

[41] J.E. Efome, M. Baghbanzadeh, D. Rana, T. Matsuura, C.Q. Lan, Effects of superhydrophobic SiO 2 nanoparticles on the performance of PVDF fl at sheet membranes for vacuum membrane distillation, Desalination, 2015, 373: 47–57.
DOI: 10.1016/j.desal.2015.07.002

[42] J. Zhang, Z. Song, B. Li, Q. Wang, S. Wang, Fabrication and characterization of superhydrophobic poly (vinylidene fl uoride) membrane for direct contact membrane distillation, Desalination, 2013, 324: 1–9.
DOI: 10.1016/j.desal.2013.05.018

[43] M. Khayet, T. Matsuura, Preparation and Characterization of Polyvinylidene Fluoride Membranes for Membrane Distillation, Ind. Eng. Chem. Res. 2001, 40: 5710–5718.
DOI: 10.1021/ie010553y

[44] D. Hou, H. Fan, Q. Jiang, J. Wang, X. Zhang, Preparation and characterization of PVDF flat-sheet membranes for direct contact membrane distillation, Sep. Purif. Technol. 2014, 135: 211–222.
DOI: 10.1016/j.seppur.2014.08.023

[45] M. Tomaszewska, Preparation and properties of flat-sheet membranes from poly (vinylidene fluoride) for membrane distillation, Desalination, 1996, 104: 1–11.

 DOI: https://doi.org/10.30564/hsme.v1i2.1346